SOLAR WIND HELIUM ABUNDANCE AS A FUNCTION OF SPEED AND HELIOGRAPHIC LATITUDE: VARIATION THROUGH A SOLAR CYCLE

Justin C. Kasper,[1] Michael L. Stevens, and Alan J. Lazarus
Kavli Institute for Astrophysics and Space Research, Massachusetts Institute of Technology, Cambridge, MA

John T. Steinberg
Space Science and Applications, Los Alamos National Laboratory, Los Alamos, NM

and

Keith. W. Ogilvie
NASA Goddard Space Flight Center, Greenbelt, MD

ABSTRACT

We present a study of the variation of the relative abundance of helium to hydrogen in the solar wind as a function of solar wind speed and heliographic latitude over the previous solar cycle. The average values of A_{He}, the ratio of helium to hydrogen number densities, are calculated in 25 speed intervals over ($\sim$27 day) Carrington rotations using Faraday cup observations from the *Wind* spacecraft between 1995 and 2005. We find that for solar wind speeds between 350 and 415 km s^{-1}, A_{He} varies with a clear 6 month periodicity, with a minimum value at the heliographic equatorial plane and a typical gradient of 1% per degree in latitude. Once the gradient is subtracted, we find that A_{He} is a remarkably linear function of solar wind speed. We identify the implied speed at which A_{He} is zero as 259 ± 12 km s^{-1} and note that this speed corresponds to the minimum solar wind speed observed at 1 AU. The vanishing speed may be related to previous theoretical work in which enhancements of coronal helium lead to stagnation of the escaping proton flux. During solar maximum the A_{He} dependences on speed and latitude disappear, and we interpret this as evidence of two source regions for slow solar wind in the ecliptic plane, one being the solar minimum streamer belt and the other likely being active regions.

Subject headings: acceleration of particles — interplanetary medium — plasmas — Sun: abundances — Sun: corona — Sun: fundamental parameters

1. INTRODUCTION

As the second most abundant element in the Sun, helium plays a significant role in the structure and dynamics of the solar wind, corona, and interior. The relative abundance of helium to hydrogen by number density, defined in this paper as $A_{\mathrm{He}} \equiv 100(n_{\mathrm{He}}/n_{\mathrm{H}})$, rarely exceeds $A_{\mathrm{He}} \sim 5$ in the steady-state solar wind, but can vary rapidly by more than an order of magnitude on timescales of minutes. In contrast to the quasi-steady solar wind, the transient interplanetary plasma associated with coronal mass ejections (CMEs) can be highly enriched in helium, with reports of $A_{\mathrm{He}} > 20$. Simple models of solar wind formation in the corona predict that the speed and flux of hydrogen should both increase sharply with heating rate in the corona, yet the hydrogen flux in interplanetary space is roughly constant and independent of speed (Feldman et al. 1978; Neugebauer 1981). Multifluid simulations attribute the near constancy of the solar wind hydrogen flux to a regulatory role played by helium in the corona (Geiss et al. 1970; Bürgi 1992; Hansteen et al. 1994, 1997). Determining the evolution of helium in these plasmas allows us to characterize our heliosphere, to improve our understanding of space weather, and to test general theories of the regulation of energy and matter in magnetized and multifluid astrophysical plasmas. In this paper, trends in the variation of A_{He} as a function of speed and heliographic latitude over a full solar cycle are reported and discussed in the context of the evolving connection between the solar interior and interplanetary space.

Indirect measurements allow us to piece together a picture of the evolution of the helium abundance from the solar core to interplanetary space. The best estimates of the abundance of helium in the solar core come from numerical simulations of the evolution of the Sun over its 4.6 Gyr lifetime. Models that assume $A_{\mathrm{He}} = 10$ in the solar core produce the best agreement with the current observed solar radius and luminosity and are also in agreement with measurements of the cosmological value of A_{He} (Guzik & Cox 1993). In the convection zone above the rigidly rotating solar core, helioseismology is used to probe the evolution of plasma parameters, such as sound speeds and composition. In the convection zone we find helium has decreased from the core value to $A_{\mathrm{He}} \approx$ 7–8. This decrease is attributed in part to gravitational settling, wherein heavier elements diffuse through the base of the convection zone into the solar core. The temperature of the solar interior decreases monotonically with radius, and at heights of 0.96 and 0.98 $R_{\odot}$ helium becomes singly ionized and neutral, respectively (Basu & Antia 1995). New helioseismic measurements of shallow waves in this region of helium recombination indicate that the abundance remains depressed at $A_{\mathrm{He}} = 8$ (Basu & Antia 1995).

Direct measurements of A_{He} on the solar surface are generally not possible because the temperature is low enough that helium is predominantly neutral and in the ground state. Photospheric helium emission has been observed during solar flares, and suggests that $A_{\mathrm{He}} \sim 8$ at the surface, similar to the values throughout the convection zone. Above the photosphere, helium becomes reionized as the temperature of the solar atmosphere rapidly rises through a narrow transition region to become the million degree solar corona. Spectral measurements of helium in the corona are

[1] Corresponding author: jck@mit.edu.

complicated by a strong photospheric nitrogen line, but several observations have been performed, revealing the startling fact that helium in the corona is rarely seen to exceed $A_{\mathrm{He}} = 4$–5. Other processes reduce A_{He} by a factor of 2 between the photosphere and the corona (e.g., Geiss 1982; Laming 2004). Numerical simulations of the evolution of helium through the complex transition region actually underestimate the observed abundances, and an artificial viscosity representing a process such as turbulent mixing is generally introduced to reproduce the observed values (e.g., Hansteen et al. 1994).

From the corona to the solar wind, the helium fraction may undergo further change. Helium does not couple as strongly to the gravitational and pressure gradients in the corona as hydrogen, so it does not directly experience the classical Parker mechanism that accelerates coronal hydrogen to supersonic speeds (Parker 1958). Instead, helium is reliant on other mechanisms for acceleration out of the corona, such as coupling to accelerated hydrogen through Coulomb collisions. In addition, helium may enter cyclotron resonance with cascading turbulent Alfvénic fluctuations in the corona, and the variable intensity of those fluctuations may account for the variability of interplanetary A_{He} (Bochsler 2000). In situ measurements of A_{He} in the solar wind can be used to gain an understanding of the sources of helium variation in the solar corona, the nature of the physics of the transition region, and the mechanisms responsible for the acceleration of the solar wind.

Early studies of solar wind A_{He} focused on the detection of solar cycle effects, since it was clear that the structure of the corona changes dramatically over the course of the 11 yr cycle of solar activity. Ogilvie & Hirshberg (1974) first reported the dependence of A_{He} on the solar cycle in a study that combined the measurements of several spacecraft. The authors identified A_{He} variation with the largest average values seen during periods of high solar activity. Feldman et al. (1978) also reported a solar cycle dependence, using data from the *IMP 6*, *IMP 7*, and *IMP 8* spacecraft. The amplitude of the modulation detected by Ogilvie & Hirshberg (1974) was equal to the scatter in the observed values of A_{He}. This might have raised questions about the significance of the result were it not for the discovery that the average value of A_{He} was additionally a function of solar wind speed. In general, it was seen that the average values of A_{He} were an increasing function of solar wind speed. The direct relationship between A_{He}, speed, and solar cycle were unclear from these observations. Ogilvie & Hirshberg (1974) claimed that the greatest speed dependence occurred near the peak of solar activity, while Feldman et al. (1978) saw the greatest effect at solar minimum. Limited statistics contributed to the difficulty in separating these three variables. The original explanation for the solar cycle dependence was that slow solar wind with low A_{He} emerges from near the heliospheric current sheet (HCS), the streamer belt, or coronal hole boundary layers (CHBLs), while fast solar wind, emerging from coronal holes, has a high helium abundance. The average value of A_{He} would then increase toward solar maximum as the average speed observed at 1 AU increased in combination with a higher rate of CMEs (Borrini et al. 1983).

More recently, Aellig et al. (2001) studied the A_{He} modulation using observations from the *Wind* Solar Wind Experiment (SWE) Faraday cup ion detectors (Ogilvie et al. 1995). That study conclusively demonstrated that A_{He} is a strong function of solar cycle, especially for solar wind speeds below 500 km s^{-1}. Aellig et al. (2001) divided the A_{He} measurements into a series of speed ranges and calculated the average value of A_{He} in 250 day intervals. For these low speeds, A_{He} was found to be at a minimum at solar minimum. During solar minimum, there was a positive correlation between A_{He} and solar wind speed. During solar maximum, A_{He} was

about 4.5 independent of solar wind speed. These new observations raised two questions. First, what would produce the strong correlation between A_{He} and speed seen during solar minimum? Second, if the correlation between A_{He} and speed seen during solar minimum results from a fundamental physical process within the corona, why does it vanish during solar maximum?

In this paper, we further examine the *Wind* A_{He} measurements with higher speed and time resolution, and extend the earlier study by adding 5 additional years of *Wind* observations. The structure of this paper is as follows. In § 2, we describe the *Wind* SWE observations. In § 3, we present an updated version of the analysis in Aellig et al. (2001). We show that the solar minimum effect observed from 1995 to 1997 is also seen in 2005. We show that beyond the general variation with solar cycle, for low speeds A_{He} is strongly correlated with the sunspot number. In § 4, we examine the solar minimum period in higher detail by calculating A_{He} over individual Carrington rotations of the solar surface. We find that at this higher time resolution, A_{He} in the slow solar wind during solar minimum is strongly modulated with a period of 6 months. This modulation is attributable to the yearly variation in heliographic latitude of the Earth and the *Wind* spacecraft. Finally, in § 5 we examine the average value of A_{He} with speed after the modulation due to the latitudinal gradient is removed and find that A_{He} exhibits a very linear dependence on solar wind speed. In addition, we show that the speed at which A_{He} vanishes corresponds to the minimum speed solar wind measured by *Wind*. In § 6 we consider theories of solar wind formation and the role of helium in the solar corona in light of these new observations.

2. HELIUM OBSERVATIONS WITH THE *WIND* SPACECRAFT

The *Wind* SWE Faraday cups measure the reduced distribution functions of solar wind hydrogen and helium along 40 angles every 92 s (Ogilvie et al. 1995). From the observations we derive bulk velocities, thermal speeds and temperature anisotropies, and number densities for hydrogen and helium by fitting the measurements with convected bi-Maxwellian distribution functions. SWE has operated nearly continuously since the launch of the spacecraft in late 1994 and has provided us with a data set spanning a solar cycle that is ideal for this study of long-term variation of A_{He}. In particular, recent studies have shown that the Faraday Cup–derived solar wind speeds are accurate to less than 1%, the absolute uncertainty in the SWE densities is less than several percent, and the drift in the density response is less than 0.1% per decade (Kasper et al. 2006). For this study, we use the bi-Maxwellian hydrogen and helium data product available from the National Space Science Data Center. We removed a small portion of data believed to be deleteriously affected by unusual non-Maxwellian distribution functions, or by the presence of interplanetary shocks. Using the publicly available MIT interplanetary shock database, shocks and any accompanying coronal mass ejections have been removed from the data set.

3. HELIUM ABUNDANCE AND THE SOLAR CYCLE

The speed-dependent variation of A_{He} over an entire solar cycle is summarized in Figure 1. The helium abundance at *Wind* is compared to the hydrogen abundance and grouped into windows according to the bulk solar wind speed. The speed ranges of the 10 windows are irregular, chosen such that the number of spectra in each window over the entire period is the same for each. The measurements in each window are then time averaged over 250 day intervals. Typically, more data are available at high speeds during solar maximum and at low speeds during minimum; however, this does not place a strong limit on this present analysis.
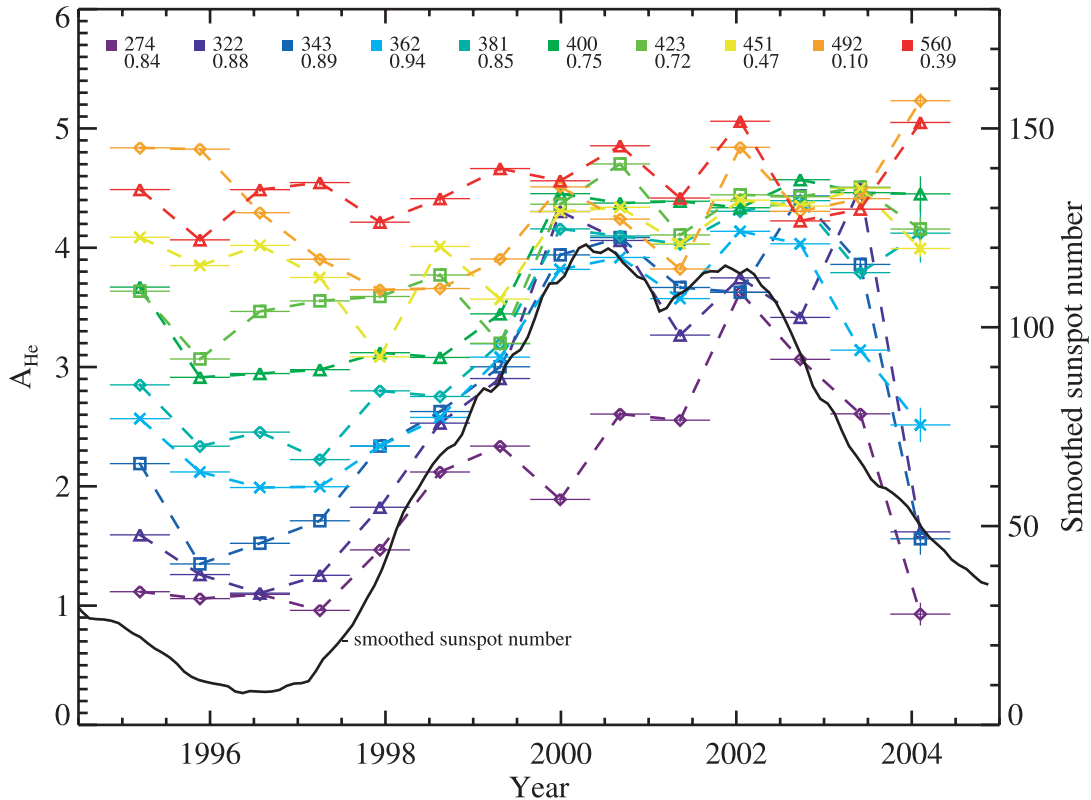
Fig. 1.—Average values of A_{He} over 250 day intervals and the smoothed sunspot number over the duration of the *Wind* mission. The legend lists the lower end of each speed window and the correlation coefficient between the averages and the smoothed sunspot number. The relative abundance of helium in the slow solar wind is strongly correlated with solar activity with a peak correlation of 0.94 for speeds between 360 and 380 km s^{-1}.

Statistical errors are calculated assuming a normal distribution of A_{He} measurements in each bin. The limitations on data availability lead to uncertainties in A_{He} of 0.16, or about 8% relatively, in the most extreme case. This uncertainty is presented in the error bars of Figure 1 and is generally too small to be seen. The relative error for a typical bin is about 0.5%, which is small compared to the overall variation with speed and time in the solar cycle.

Figure 1 is similar to Figure 2 of Aellig et al. (2001), which showed the speed-dependent A_{He} ratio covering half a solar cycle, averaged over 250 day periods from 1996 to 2000. In that study, *Wind* measurements of A_{He} were divided into seven regular velocity windows: one for $V < 350$ km s^{-1}, one for $V > 650$ km s^{-1}, and five windows, each 50 km s^{-1} wide, for the intervening speeds. Typically, the averages constituted tens of thousands of individual measurements. Figure 1 presents our extension of that earlier work through solar maximum and into the onset of solar minimum in 2004.

Figure 1 shows that the correlation between A_{He} and sunspot number is strongest at low V, consistent with the earliest studies (e.g., Ogilvie & Hirshberg 1974). It also shows that A_{He} is an increasing function of V throughout the entire solar cycle. The overall change in A_{He} between solar minimum and solar maximum is $\Delta A_{He} = 1.394 \pm 0.004$. The effect is more pronounced in the lower speed windows, where $\Delta A_{He} \sim 3$ over the solar cycle. For the window centered at 274 km s^{-1}, the connection between A_{He} and the smoothed sunspot number is strongest, with a correlation coefficient r of 0.84. At 274 km s^{-1}, A_{He} at solar maximum is 3.6 times its value at solar minimum. At high speeds, however, there is significantly less correlation between A_{He} and sunspot number. The variance of A_{He} at 560 km s^{-1}, for example, is approximately 1, and r decreases to 0.39. The positive correlation between A_{He} and solar activity decreases sharply with increasing speed across the 451 km s^{-1} window and the two adjacent windows. The total r for $V < 451$ km s^{-1} is 0.90, while the total $r = 0.29$ for faster wind.

We find the observed helium abundance is a relatively well-ordered function of wind speed during the present solar minimum, as it was during the previous. At the time of minimum sunspot number in 1996, the 250 day average A_{He} was an increasing function of V, with $r = 0.96$. In 2004 the strong speed dependence returned, demonstrating the repeatability of this phenomenon. At solar maximum, the difference in A_{He} from one speed window to the next is on the order of the variance, but a trend of increasing A_{He} with bulk speed is still seen, with $r = 0.84$. Although A_{He} varies over a more narrow range during solar maximum, the positive correlation between A_{He} and V is nonetheless present over the entire solar cycle.

4. CARRINGTON AVERAGES AND A 6 MONTH MODULATION

We have shown that A_{He} is a strong function of speed during solar minimum. In order to better characterize this dependence and to identify other factors that may regulate A_{He}, we have increased both the time and speed resolution of the previous analysis. We define 25 speed windows of varying width such that over the course of the *Wind* mission an equal number observations fall into each interval. The typical width of a speed window is 10 km s^{-1}, but the highest speed windows are 50 km s^{-1} wide. Instead of 250 day intervals, we separated the data into individual Carrington rotations of the Sun. Averaging over Carrington rotations reduces our sensitivity to structures at particular longitudes
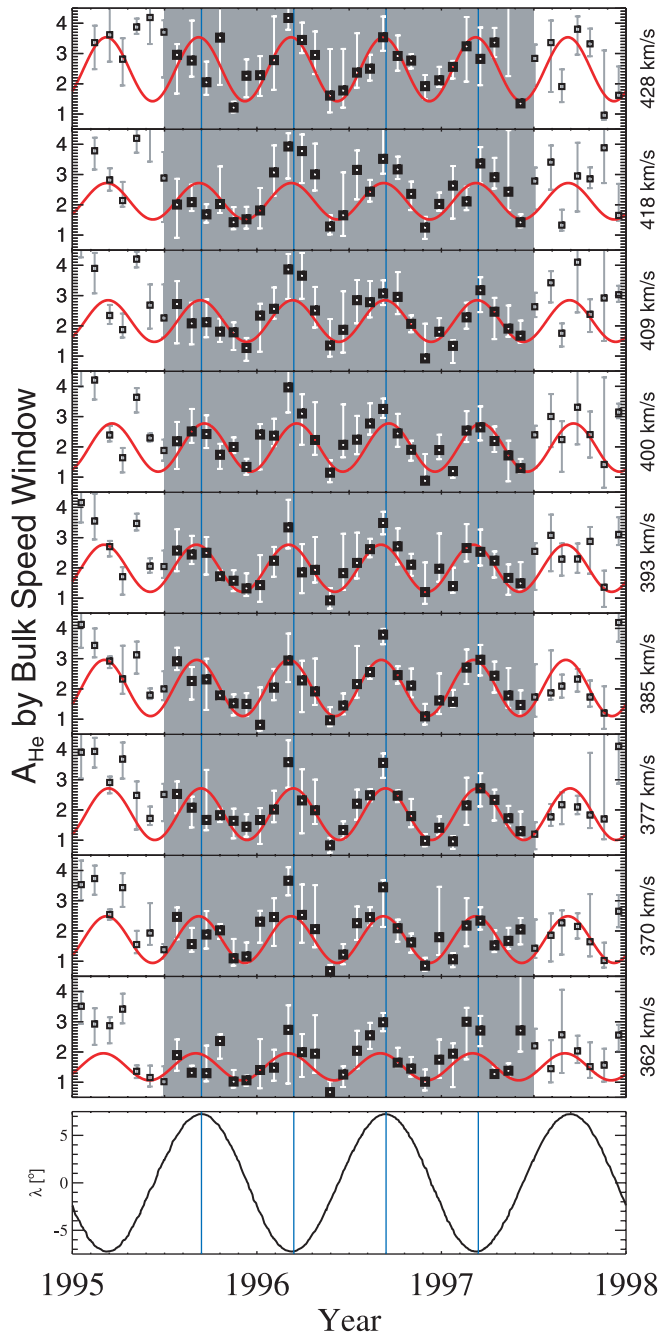
Fig. 2.—Averages of A_{He} over Carrington rotations for nine narrow speed intervals over a 3 yr period from 1995 through 1998. Bold symbols, occurring during the 2 years of minimum solar activity, exhibit a clear modulation with a 6 month period. The bottom panel is a plot of the heliographic latitude of Earth and the *Wind* spacecraft. Maxima in A_{He} occur when the spacecraft is farthest from the heliographic equator.

in the solar corona and provides us with a significant number of measurements in each speed window.

Figure 2 shows the results of examining the Carrington rotation averages for nine of the speed windows. For speeds ranging from 360 to 430 km s^{-1} during the 2 yr interval surrounding solar minimum, from mid-1995 through mid-1997, there is a significant modulation of A_{He}, with a period of 6 months. In the figure, each square represents the average value of A_{He} in a Carrington rotation. The centers of the speed windows are indicated on the right side of the plot. Measurements between mid-1995 and mid-1997 are highlighted, with error bars indicating the 16th and 84th

percentiles of the A_{He} distribution in each bin. The 6 month modulation appears related to Earth's (and *Wind*'s) annual variation in heliographic latitude, as we describe later. But first we consider the validity of the modulation seen in Figure 2.

The range of speeds in which modulation is significant was identified by calculating a Lomb-Scargle (LS) normalized periodogram for each time series and identifying the period and significance of the strongest periodic signal (Press et al. 2002, § 13.8). The LS test is a method of spectral analysis for comparing the hypothesis that an irregularly sampled data population represents a significant periodic signal against the hypothesis that it represents random noise. For the speed windows shown in Figure 2, it was verified that there is a statistically significant 6 month periodic modulation for each window. In each velocity bin, the Lomb-normalized periodogram, which is analogous to the power spectrum, is calculated for the Carrington-averaged A_{He} ratio. The maximum value, corresponding to the strongest periodicity present in the data, is obtained, along with the associated "false alarm" probability, also called the significance value, s. In this calculation, low s implies a high probability that the periodicity is present in the signal. For windows in which the best significance value is less than 0.2, corresponding roughly to 80% confidence or better, we fit A_{He} to a sinusoid function using least-squares fitting:

$$A_{He} = A_{He}(V) + \Delta A_{He} \cos\left(\frac{2\pi(t - t_0)}{T}\right). \qquad (1)$$

Here, $A_{He}(V)$ is the constant component, and the free parameters are the amplitude of the modulation, ΔA_{He}, the period of modulation in years, T, and a phase offset, t_0, also in years.

Fitting these data analytically and assessing the fit validity presents a challenge. We note that the error bars shown in Figure 2 are large compared to the modulation signal. Estimating the error of the average value of A_{He} in each bin is a challenge, because the underlying distribution of A_{He} is not drawn from a single distribution function. Homogeneous streams or groups of streams that dominate a given speed window over an entire solar rotation are rare. Rarer still are streams for which A_{He} is Gauss-normal for periods on the order of the Carrington rotation period. By averaging over the rotation period, features are smoothed out to some extent, but not to such an extent that the standard error on the mean is a good description of the statistical uncertainty in a given bin. The distribution of A_{He} over a given window and time period is occasionally symmetric about a single peak, suggesting that there is a statistically simple and possibly Gauss-normal, log-normal, or kappa process. More commonly it is complex, with multiple asymmetric peaks. For this reason, we estimate typical values for a given bin and time period by taking the median and the 68% confidence levels about that median. When the data are well described by theory, an unusually small χ^2 per degree of freedom, χ^2/ν, is therefore expected, which is a simple consequence of neglecting the underlying structure of the A_{He} distribution function.

We found that for $V < 360$ or $V > 430$ km s^{-1} a constant value could fit the observations just as well as the model in equation (2). For higher speed bins, the limited data availability contributes to poorly defined Carrington averages during solar minimum, and the resulting random variance obscures any periodic trend that might be present. For $V < 360$ km s^{-1}, no periodic sources of variance are detected. For 360 km s$^{-1} < V < 430$ km s^{-1}, however, a clear periodic trend emerges over the 2 yr centered at solar minimum. In each case, T is very close to 6 months and ΔA_{He}
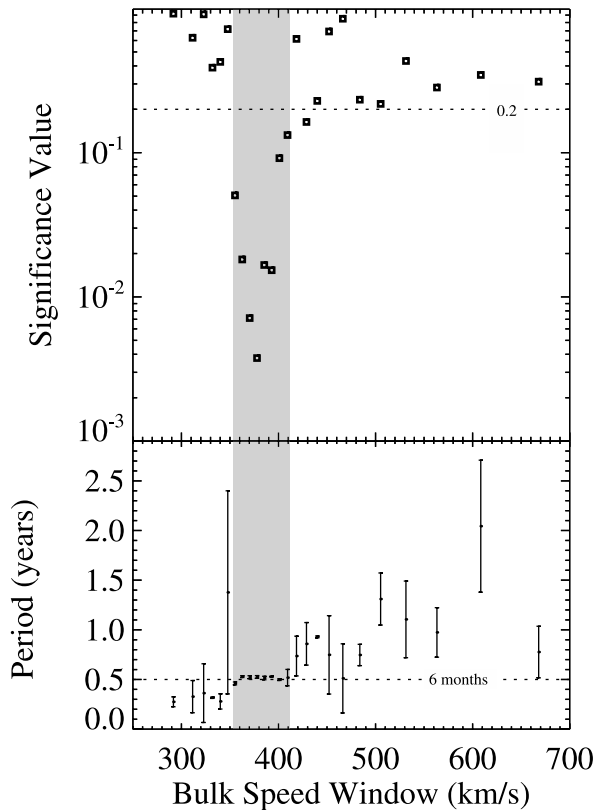
Fig. 3.—LS analysis of the significance of A_{He} fluctuations as a function of solar wind speed. The top panel is a plot of the significance and the bottom panel is a plot of the period with error bars. Low significance values correspond to high probability that a real periodic trend is present in the data. The significant modulation has a period of half a year and occurs for speeds between 350 and 410 km s^{-1}.

Fig. 4.—*Top*: Plot of the constant and modulated components of A_{He} as a function of solar wind speed. The modulated component is highlighted in both panels with a light gray band. The dotted line is the best fit to the slow speed component, which omits the three highest speed points. The fit for slow wind projects that A_{He} goes to zero at a proton speed of 259 ± 12 km s^{-1}. This vanishing speed is indicated in both panels with a dark gray band. *Bottom*: Histogram of all solar wind speeds measured by *Wind* over the course of its mission. Within 1 σ of the helium vanishing speed, the frequency of solar wind observations drops by 3 orders of magnitude.

ranges between 0.7 and 1. A bootstrap calculation was performed to give crude estimates for the parameter errors. Choosing the bin centered at 370 km s^{-1} as a typical example, $T = 6.33 \pm 0.21$ months and $\Delta A_{He} = 0.8 \pm 0.1$ at a confidence of 95%. This bin happens to be relatively small, since data availability in this speed range is very good. As one would expect, χ^2/ν is a bit lower than unity when the LS confidence is high; in this case it is 0.29. The periodic trend is also quite clear in larger bins up to about 430 km s^{-1}. The 411–421 km s^{-1} bin is fit by a sinusoid with $T = 6.2 \pm 0.21$ months and $\Delta A_{He} = 0.7 \pm 0.1$ at a confidence level of 94%.

This analysis is summarized in Figure 3, which shows the significance values and periods for the entire data set. Every fit with confidence greater than 80% has the same 6 month period and is in phase. The common phase is such that the helium abundance peaks at the end of February and July each year. Due to the tilt of the ecliptic plane relative to the solar equatorial plane, the heliographic latitude of *Wind* ranges from about +7.25° in early March to −7.25° in early September. Examination of Figure 2 clearly indicates that A_{He} increases as Earth moves farther north or south of the heliographic equator.

5. SPEED GRADIENT AND THE MINIMUM SPEED OF THE SOLAR WIND

Figure 4 shows the baseline value of A_{He} as a function of V once the variation due to the latitudinal effect is removed, based on the analysis discussed in the previous section. For speed windows in which the latitudinal variation has been shown to be significant,
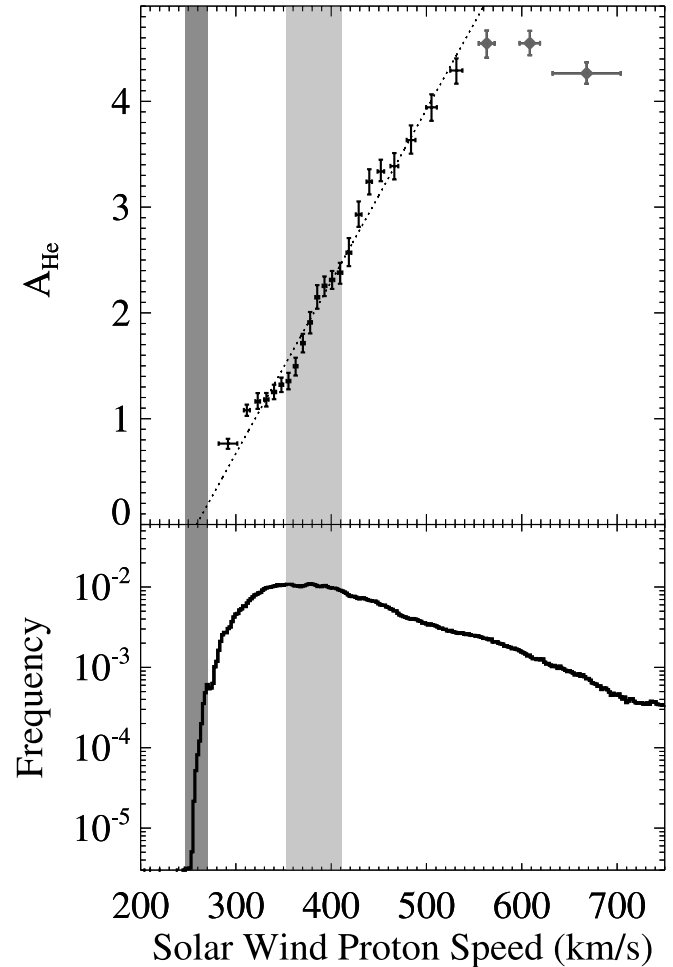
the A_{He} abundance is represented by the baseline constant term $A_{He}(V)$ in equation (2). In windows in which no significant periodic variation is detected, a simple statistical average is plotted instead. An important simplifying assumption is made for speed windows in which the periodicity is significant. The sinusoidal fits are imperfect because the statistical errors have been overestimated, as discussed in the previous section. We assume for the analysis in this section, however, that sinusoids are a correct model, and that these overestimations are the primary source of uncertainty for the derived baseline and modulation amplitudes. If this assumption is correct, the χ^2/ν of each successful fit can be renormalized to unity. The fit parameter uncertainties are then adjusted accordingly, and the error in $A_{He}(V)$ used in Figure 4 is based on this assumption.

The helium abundance baselines and averages plotted in Figure 4 demonstrate a monotonically increasing regime in A_{He} versus V that is remarkably linear below 530 km s^{-1}. Above this speed, A_{He} levels off, but the variation is difficult to quantify due to the large ∼50 km s^{-1} speed windows arising from low statistics. The light gray shading highlights the region where the sinusoidal

modulation is significant. We fit the A_{He} value below 530 km s^{-1} to a line,

$$A_{\mathrm{He}}(V) = G(V - V_0), \qquad (2)$$

where $G = dA_{\mathrm{He}}/dV$ is the gradient of A_{He} with speed and V_0 is the critical solar wind speed at which $A_{\mathrm{He}} = 0$. The line of best fit to the data has $G = (1.63 \pm 0.04) \times 10^{-2}$ (km s^{-1})$^{-1}$ and $V_0 = 259 \pm 12$ km s^{-1}, with $\chi^2/\nu = 1.93$. The dark gray band on the left side of Figure 4 indicates V_0, the minimum observed solar wind speed, and a 1 σ confidence interval. The bottom panel of Figure 4 is a histogram of every measurement of V from the *Wind* SWE experiment over the interval from 1994 November to 2004 March. The number of observations drops by 3 orders of magnitude within 1 σ of V_0. Bulk speeds below this band are rarely observed at 1 AU, even though it lies well above the gravitational escape speed. Over the 10 years examined, there have been less than 100 such observations in all. It would appear that A_{He} and the solar wind itself independently vanish at approximately 259 km s^{-1}.

6. DISCUSSION

The observed trends in A_{He} as a separate function of solar wind speed, heliographic latitude, and solar cycle reported in this paper place strong constraints on theoretical models of solar wind formation and coronal structure. In this section, we examine the latitude and speed gradients, and the variation of A_{He} over the solar cycle, in terms of coronal theories. This discussion is divided into five parts. In § 6.1 we consider the effects of the solar wind expansion profile on A_{He}. In § 6.2, we explore the possibility that the latitudinal gradient in A_{He} is due to differential flow between hydrogen and helium. Next, we consider models of composition variation within coronal magnetic loops in § 6.3. We then describe previous numerical simulations that have produced associations between the helium depletion in the solar wind and limits to solar wind acceleration in § 6.4. Finally, in § 6.5 we show how our observations imply that there are two source regions of slow solar wind. Both regions exist in the corona throughout the solar cycle, but have access to Earth in different proportions as the coronal field evolves.

6.1. *Effect of the Solar Wind Expansion Profile on A_{He}*

Classically, the fact that A_{He} increases with speed during solar minimum has been interpreted as confirmation of the traditional view that fast solar wind emerges from CHs and slow solar wind emerges from either the streamer belt or the polar CHBL. That interpretation rests on interplanetary observations of decreased values of A_{He} near the HCS, the superradial divergence of the magnetic field of the current sheet in the corona, and the coupling between the expansion of the coronal field and the flux of protons. Helium is not efficiently accelerated by the Parker mechanism, and instead relies on coupling to the accelerated coronal hydrogen through Coulomb drag.

Consider the variation of the proton flux due to the expansion of the coronal field. The Wang & Sheeley (1990) convention is used to describe the divergence of the coronal magnetic field in terms of the flux tube expansion factor, f_s:

$$f_s \equiv \left(\frac{R_\odot}{R_s} \right)^2 \frac{B(R_\odot)}{B(R_s)}, \qquad (3)$$

where $B(R_s)$ is the strength of the field at a source surface at height R_s and $B(R_\odot)$ is the strength of the field at the corresponding

footpoint at the base of the corona. This factor has been linked to the acceleration of solar wind in the corona by Levine et al. (1977), who hypothesized that high-speed solar wind originates in coronal regions with minimum flux-tube expansion ($f_s < 1$) and slow solar wind emerges from coronal streamers in which the field diverges rapidly ($f_s > 1$). In general, they predicted that the bulk speed should be inversely proportional to the expansion factor,

$$U \propto f_s^{-1}. \qquad (4)$$

Although the flux of protons at 1 AU is nearly constant, it varies by as much as an order of magnitude in the acceleration region (below $\sim 2.5\ R_\odot$), where the plasma β is low and the expansion profile is far from radial (Wang & Sheeley 1990). In this region, the proton flux is enhanced in proportion to f_s^{-1}. Also deep in this region, the fluxes of different species are coupled via Coulomb collisions, which tend to transfer momentum from protons to α-particles. The efficiency of this coupling is a highly nonlinear function of the fluxes of each species. While the force balance involves more detailed considerations, it is essentially correct to say that α-particles, which have a stronger tendency toward gravitational settling than protons, are dependent on this coupling to escape the corona. Aellig et al. (2001) argued that in this way the proton flux variation in the acceleration region ultimately determines the A_{He} variations seen at 1 AU. It was hypothesized that the reduction of proton flux at latitudes with an overexpanding magnetic field reduces the efficiency of the Coulomb drag for transferring momentum to helium. In that picture, the abundance and the proton velocity are signatures of the same magnetic profile. A representative expansion profile for the slow wind at solar minimum was inferred by Wang (1994), and used by Aellig et al. (2001) to show that the correlation between A_{He} and V at 1 AU was consistent with this theory at particular points in the solar cycle. Near the HCS, the expansion is particularly large, so one would expect to see slow, helium-poor wind at HCS crossings. At higher latitudes, as the overexpansion decreases, one would expect faster, more helium-rich wind. This is illustrated in Figure 5, which gives examples of the source-surface magnetic field at solar minimum and the irregular magnetic field measured at solar maximum, as deduced from Wilcox Solar Observatory magnetograms. During solar minimum, the HCS lies in the equatorial plane and structures are ordered by latitude.

Our observations at solar minimum support the expansion-profile hypothesis, but also indicate another level of complexity. Figure 1 shows that A_{He} is clearly correlated to wind speed at solar minimum, and more loosely so throughout the solar cycle. The correlation between wind speed and heliographic latitude during solar minimum has been demonstrated using the first *Ulysses* fast latitude scan in 1994/1995 (McComas et al. 2003 and references therein). The key observation here, however, stems from the fact that the wind speed is not perfectly determined by heliographic latitude. Instead, a range of wind speeds can be seen at all of the near-ecliptic latitudes in this study. Likewise, the full range of observed speeds is seen to some degree at latitudes accessible to *Wind*. While the previous argument dictates a large-scale trend in A_{He}, V, and f_s, all determined by the heliographic latitude, it is insufficient to explain the full range of observations seen near the ecliptic. As was shown in Figure 3, when we examine A_{He} with the proton speed fixed, a distinct latitude dependence remains for a commonly occurring range of speeds. Thus, A_{He} cannot be a function of the f_s alone at solar minimum.

It has been hypothesized that the signature of the HCS at 1 AU includes a minimum in the relative helium abundance (Borrini
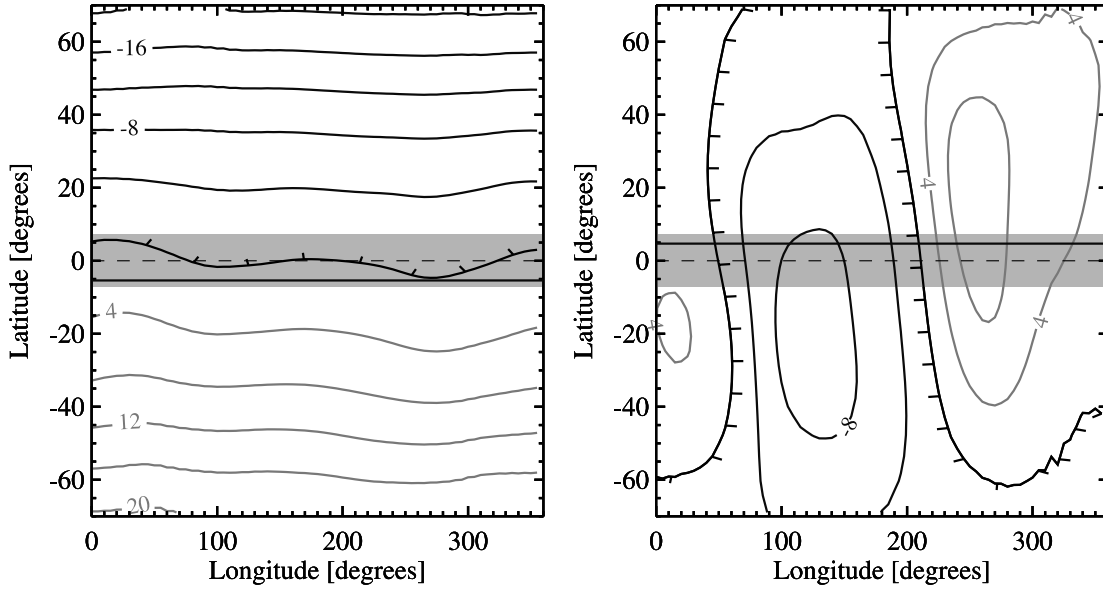
Fig. 5.—Demonstration of the evolution of the structure of the coronal magnetic field over the solar cycle. Photospheric field measurements from Wilcox Solar Observatory are extrapolated onto a surface 2.5 $R_\odot$ into the corona using a force-free potential model. Contour plots of the radial component of the magnetic field at the surface are shown for solar minimum using measurements collected in 1995 December (*left*) and for solar maximum using measurements from 2000 June (*right*). Selected contours indicate the strength of the radial component in gauss, and the neutral line is the black line with ticks. The horizontal dashed line is the heliographic equator, the horizontal solid line is the heliographic latitude of *Wind* at each time, and the gray region is the range covered by the Earth over the course of 1 yr. Note that during solar minimum *Wind* slowly moves across the neutral line, while during solar maximum the mapping is more complex.

et al. 1981). A reorganization of the *Wind* solar minimum observations does provide evidence that the super-radial expansion of the magnetic field at the HCS in the corona can significantly reduce the interplanetary A_{He}. In Figure 6, we plot the same data used in calculating the latitudinal gradients in § 4, but now averaged over nine intervals in heliographic latitude with different colors representing different speeds windows. The latitude gradient reported in § 4 is clearly present, and appears well fit by a quadratic for moderate speeds, as illustrated by the blue line. A_{He} generally takes on different values for different speed windows at each latitude, but an exception occurs closest to the heliographic equatorial plane. Here, the A_{He} values converge in all speed windows, within error, to a single value of $A_{\mathrm{He}} \sim 1.5$. This convergence may in fact be the true signature of the direct role of the HCS in diminishing A_{He}, regardless of *V*.

6.2. *Latitudinal Variation as a Signature of Differential Flow*

A possible interpretation of the latitudinal variation of A_{He} is that it is due to differential flow between helium and hydrogen in the corona that has been washed out by the time the plasma reached 1 AU. Helium is generally observed to have a larger velocity then than hydrogen, especially in the fast solar wind (e.g., McKenzie et al. 1978; Marsch et al. 1982a, 1982b; von Steiger et al. 1995). This phenomenon is probably an artifact of wave-resonant heating and acceleration in the corona (e.g., Dusenbery & Hollweg 1981; Tu et al. 2003). Plasma instabilities are believed to limit the differential flow to the local Alfvén speed (Xing & Habbal 2000; Araneda et al. 2002), and it has been shown that Coulomb drag slowly reduces the differential flow as the solar wind evolves (Neugebauer 1976). *Wind* observations of differential flow between hydrogen and helium have been reported previously (Steinberg el al. 1996; Kasper et al. 2006). Here we make a simple conservation argument to show that A_{He} variation is consistent with source-surface variation of these acceleration processes.

The differential flow speeds observed at 1 AU are small relative to the Alfvén speed at the source surface. A simple particle conservation argument shows that as Coulomb drag drives the helium and hydrogen toward a single bulk flow speed, the relative abundance of the helium is enhanced to a degree that is consistent with observation. Consider the flow of hydrogen and helium along a one-dimensional flux tube with cross-sectional area *S*. Denote the density of helium n_{He}, the density of hydrogen n_{H}, and the respective speeds V_{He} and V_{H}, with $\Delta V = V_{\mathrm{He}} - V_{\mathrm{H}}$. Denote quantities at a source surface within the corona with subscript 0 and quantities at 1 AU with subscript 1. In steady state, particle conservation relates the density of the two species through

$$S_0 V_{\mathrm{H},0} n_{\mathrm{H},0} = S_1 V_{\mathrm{H},1} n_{\mathrm{H},1}, \tag{5}$$

$$S_0 V_{\mathrm{He},0} n_{\mathrm{He},0} = S_1 V_{\mathrm{He},1} n_{\mathrm{He},1}. \tag{6}$$

So the helium abundance ratio at 1 AU is given by

$$A_{\mathrm{He},1} = \frac{\left(1 + \Delta V_0 / V_{\mathrm{H},0}\right)}{\left(1 + \Delta V_1 / V_{\mathrm{H},1}\right)} A_{\mathrm{He},0}. \tag{7}$$

In the slow wind at 1 AU, ΔV_1 is small compared to $V_{\mathrm{H},1}$ on average (e.g., Kasper et al. 2006). If we assume that the high Coulomb collision rates and the longer propagation times for slow solar wind result in negligible differential flow at 1 AU, then the interplanetary A_{He} observed by *Wind* is directly proportionate to the differential flow at the source surface:

$$A_{\mathrm{He},1} \propto \left(1 + \frac{\Delta V_0}{V_{\mathrm{H},0}}\right) A_{\mathrm{He},0}. \tag{8}$$

If the source surface abundance is indeed uniform, then the values of the $\Delta A_{\mathrm{He}} / A_{\mathrm{He}}$ observed at low speeds are consistent with small differential flow in the corona at the heliographic equator increasing to $\Delta V_0 / V_{\mathrm{H},0} = 0.5$–1 at higher latitudes. These values
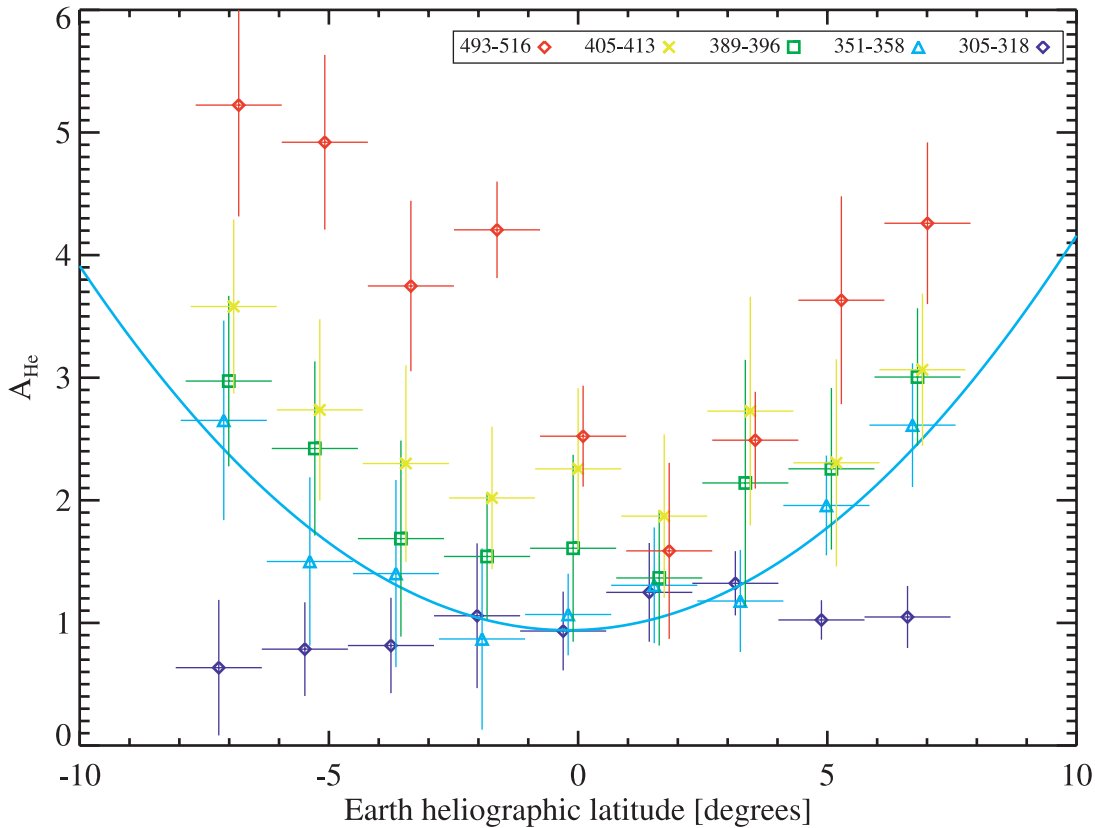
FIG. 6.—Plot of average helium abundance as a function of heliographic latitude for five selected solar wind speeds. The light blue symbols are for solar wind speeds between 351 and 358 km s^{-1}, and are an example of a speed interval with the clearest sinusoidal modulation. Plotted against latitude, the average values of A_{He} are well modeled as a quadratic function of latitude. At higher speed solar winds, the parabolic function is no longer observed, although there is still a minimum in A_{He} near the heliographic equator. Of note is the fact that separated for latitude there is an interval where A_{He} is a weak function of solar wind speed with an average value of approximately 1.2%.

are consistent with estimates of the coronal Alfvén speed, and imply a latitudinal gradient in the strength of the wave-resonant processes associated with differential flow in the solar minimum corona. It is not unreasonable to require that heating by cyclotron-resonant Alfvén wave absorption, for example, not be uniform at the base of the corona. Small-scale reconnection in the chromospheric network of magnetic loops is one possible source of significant wave power for coronal heating and solar wind acceleration and has been shown to be highly nonuniform (Tu & Marsh 2001). These reconnection events, or any other significant source of Alfvén waves, would seed a turbulent spectrum of fluctuations that becomes resonant with low Larmor frequencies at relatively high wave powers. At solar minimum, the surface flows and magnetic topology low in the corona are well ordered with heliographic latitude, so we might expect to see simple emergent behaviors at 1 AU. This would not be the case at solar maximum, where a wide variety of observational techniques have shown that the coronal magnetic structure and flows are not simple or steady state.

6.3. Abundance Variations within Loop Confinement Models

It has also been hypothesized that the composition, speed, and other properties of solar wind plasma are determined in part by the confinement of the plasma in small-scale closed magnetic structures prior to release. In this picture, the properties of plasma confined to magnetic loops deep in the corona change gradually over the duration of confinement until the plasma is released via reconnection with open field lines (Fisk 2003). This perspective generalizes observations of large coronal loops down to below observable scales. Qualitatively, it is expected that the confinement time of plasma to a coronal loop is related to its physical size, and these factors in turn determine the temperature profile and the timescale for wave absorption, gravitational settling, radiation, and kinetic processes (Woo 2004; Fisk 2003).

As pointed out previously, there is no direct way to measure the value of A_{He} or the uniformity of it in these coronal loops. Assuming that the loop reconnection model is valid, our observation that the helium abundance of the solar wind is an increasing function of proton bulk speed implies that loops associated with low speeds have some mechanism for shedding helium relative to those associated with higher speeds. One possibility is that high-speed streams follow from smaller, shorter lived loops whose elemental abundances are set deep in the photosphere, where low first ionization potential (FIP) elements are more likely in an ionized state. Low-speed streams, by contrast, may come from loops extending to high altitudes and thus lower temperatures for comparatively long confinement times. In such loops, gravitational settling of heavy ions may become significant. A recent study by Endev et al. (2005), however, indicates that the opposite may be the case. This work modeled helium release from closed-field regions by simulating a hydrogen-helium magneto-hydrodynamics (MHD) plasma in a pinched, one-dimensional flux tube. For confinement times of several days, this simulation found that closed-field regions become enriched with helium, accumulating gradually deeper in the corona. When these flux tubes are opened, a delayed outflow of helium-rich material and a reduction in the proton flux follows over timescales on the order of the confinement time. The delay in helium release was also

shown to increase with increasing confinement time. The observations presented here provide simple constraints on the coupling of the wind speed and A_{He} for the ongoing development of loop-confinement models.

6.4. Multifluid MHD Models and the Minimum Speed of the Solar Wind

By extrapolating the curve in Figure 4, we showed that the total depletion of helium coincides with the "speed limit" for the slow solar wind at $V_0 = 259$ km s^{-1}, as defined in equation (2). Theoretical work on the relationship between properties of the solar corona and the final speed of the solar wind to date has generally involved scaling relationships between coronal temperature or energy flux with no implied lower bound in speed (Fisk 2003; Schwadron et al. 2006). We hypothesize that this coincidence indicates a critical behavior in the solar corona wherein helium accumulation inhibits the bulk acceleration of the solar wind. Several theoretical models, such as those of Bürgi (1992), Hansteen et al. (1994), and the aforementioned Endev et al. (2005), have demonstrated the moderating influence of helium abundance and drag between ion species on solar wind acceleration. These models predict that thermal forces create an enhancement in helium near the coronal temperature maximum, and that the friction force between α-particles and protons throughout moderates the flux of protons in the solar wind. A three-fluid MHD simulation by Hansteen et al. (1994) also found that, for an isothermal corona model below a critical temperature, the α-particle radial speed can become negative, leading to nonequilibrium solutions with runaway decreases in proton and α-particle flux. In a simplified isothermal corona model, a critical proton flux is predicted below which helium accumulates in the corona and proton and α-particle flux decrease without bound. Endev et al. (2005) also envisions a helium-pooling process wherein the confinement time exceeds the release time for closed regions. The speed limit that we observe for the slow solar wind may likewise indicate a speed below which the frictional impulse from protons is no longer sufficient to drag α-particles out of the corona. Alternatively, the speed may correspond to a loop-evolution scenario in which the confinement time becomes too long for α-particles to be sufficiently heated and escape upon transient reconnection with open field lines. The subsequent accumulation of α-particles in the corona in either scenario could create a bottleneck that further suppresses the flow of both species until some other mechanism restores equilibrium. In addition to explaining the minimum speed of the quiescent solar wind, this regulatory role of helium in the corona may also explain why many CMEs exhibit enhanced A_{He}.

6.5. Multiple Sources of Slow Solar Wind

At solar maximum, the regularity of the magnetic expansion profile breaks down and the mixture of different solar wind sources at the same latitude becomes significant. To this point, we have avoided speculation on the source surface latitudes and structures that give rise to slow solar wind, except to note the possible signature of the HCS and to acknowledge that wave heating and magnetic topology probably differ in the polar coronal hole and polar coronal hole boundary relative to the rest of the Sun. The overall increase in A_{He} in the slow solar wind with increasing solar activity leads us to re-examine the source question. Why is A_{He} correlated with sunspot number in the slow solar wind and not in the fast wind? Why is the latitude-independent contribution to A_{He} less strongly correlated with speed at solar maximum? To answer these questions, we hypothesize that there are two sources of slow solar wind. One source is associated with the streamer belt, but not necessarily the HCS. It is this source that we
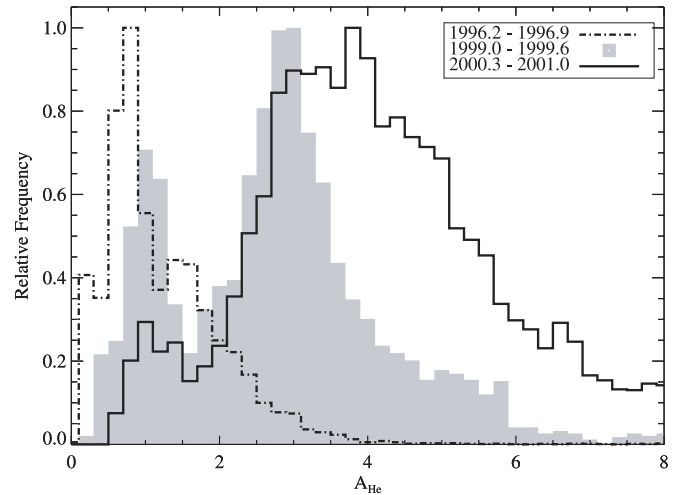

Fig. 7.—Histograms of the distribution of A_{He} for solar wind with speeds between 300 and 325 km s^{-1} during solar minimum (mid-1996; *dot-dashed line*), increasing solar activity (1999; *gray shading*), and solar maximum (2001; *solid line*). Instead of a simple increase in the observed value of A_{He} with solar activity, the distribution appears bimodal. Even at solar maximum a small population at the solar minimum value of A_{He} is seen.

see primarily over solar minimum, with the signature of the HCS noted in Figure 6. The second source region, appearing at solar maximum, is most naturally the active regions that appear and migrate to lower latitudes over that period. Note that for the slow solar wind, below 450 km s^{-1}, the average correlation coefficient of 0.84 marks a strong relationship between helium abundance and solar activity. Above 450 km s^{-1}, however, the correlation drops sharply. In the fast solar wind, the average correlation coefficient of 0.25 indicates little variation with solar activity. If slow wind with high A_{He} comes from active regions, this would explain the increase as a function of sunspot number. If slow wind with low A_{He} is associated with the streamer belt, then the disappearance of the latitudinal gradient is simply due to the fact that the HCS is no longer aligned with the heliographic equator during solar maximum.

There have been attempts to map the solar wind back to the Sun; these studies find that in some cases, the solar wind emerges from active regions (Liewer et al. 2004). It appears most likely that the slow solar wind originates from a combination of these two regions in different proportions as a function of time in the solar cycle. We looked more closely at a speed interval with many observations to address this question. Figure 7 is a series of histograms of A_{He} for solar wind speeds between 322 and 343 km s^{-1}. The histograms are taken from solar minimum in mid-1996, early 1999, and solar maximum in late 2001. The high-A_{He} peak seen here emerges in proportion to the sunspot number, and disappears altogether at solar minimum. Note also the low-A_{He} peak at solar minimum, which is still seen in the transition period and again at a very low level even at solar maximum. This suggests that the solar minimum source is still accessible to the ecliptic plane throughout the cycle, although not as often near maximum. The reduction of this source at solar maximum may reflect its association with the HCS, which becomes quite warped and may thus be less often accessible near the ecliptic at 1 AU. To test these hypotheses, more work is required to map the solar wind plasma back to the source.

7. CONCLUSIONS

We have studied the variation of helium in the solar wind using measurements from the *Wind* spacecraft. This study extends the findings of previous works by looking at A_{He} in Carrington

rotation averages, and yields the following constraints on models of solar wind formation and coronal structure.

At solar minimum, proton speed and A_{He} are correlated. This was seen in the previous cycle, and is now repeating in the present cycle. Over a range of speeds, the A_{He} increases with heliographic latitude at solar minimum, with typical gradients of $\Delta A_{\mathrm{He}} = 0.7–1$ over $7.25°$ in latitude and with minimum values in the equatorial plane. This latitude effect could possibly be a signature of a gradient in the differential flow of helium in the corona as a function of distance from the boundary of coronal holes. There is a speed-independent drop in the helium abundance to $A_{\mathrm{He}} = 1.5$ in the heliographic equatorial plane at solar minimum, likely due to the equatorial alignment of the HCS. This evidence suggests that the HCS indeed reduces the final value of A_{He}, but that the expansion of the coronal magnetic field is not the sole factor regulating the escape of helium. Future theoretical work should investigate mechanisms for the latitudinal gradient and why the gradient is only observed for solar wind speeds greater than ~360 km s^{-1}. For example, in § 6.2 we suggested that the gradient could be due to differential flow between hydrogen and helium in the corona that dissipates by 1 AU. Is it possible that there is an insufficient density of Alfvénic fluctuations to impart a differential flow in the corona where very slow wind emerges during solar minimum? In § 6.3 we discussed models of helium stratification in coronal loops. Is there a critical phenomenon in coronal loops responsible for speeds less than ~360 km s^{-1} that prevents the latitudinal gradient from being established?

While the underlying physics dictating the acceleration of helium in the corona is complex and nonlinear, after the latitudinal gradient is removed the solar minimum A_{He} is an extremely linear function of the final speed of the solar wind. This suggests that simple relationships link the efficiency of coronal hydrogen and helium acceleration. The speed gradient is $(1.63 \pm 0.04) \times 10^{-2}$ (km s^{-1})$^{-1}$, and the extrapolated speed at which there is no helium in the solar wind is $V_0 = 259 \pm 12$ km s^{-1}. This speed V_0 corresponds within 1σ to the minimum observed speed of the solar wind at 1 AU, suggesting that enriching the corona with helium may produce a lower limit in the speed of the escaping solar wind. This observation stresses the role coronal helium plays in regulating the final flux of solar wind protons and highlights the need for additional studies on the physics responsible for the minimum speed of a stellar wind. The hypothesis that high coronal A_{He} prevents the escape of coronal plasma may also be related to the fact that CME ejecta are often highly enriched in helium.

Finally, observations over the solar cycle clearly suggest that there are two sources of slow solar wind in the equatorial plane, one of which dominates at solar minimum and is associated with the streamer belt and another at solar maximum that is highly correlated with the number of active regions. Measurements of A_{He} should be combined with models that map the solar wind back to the corona to identify these sources. An accurate mapping would permit a study of A_{He} as a function of a more physical quantity than the spacecraft heliographic latitude, such as the distance from the streamer belt or coronal hole boundaries. Perhaps it could then be shown that spatial gradients in A_{He} persist through 1997 as the streamer belt becomes tilted relative to the heliographic equator. Furthermore, if it is accepted that there are two source regions, measurements of A_{He} may be used to validate these mapping methods.

REFERENCES

Aellig, M. R., Lazarus, A. J., & Steinberg, J. T. 2001, Geophys. Res. Lett., 28, 2767
Araneda, J. A., Viñas, A. F., & Astudillo, H. F. 2002, J. Geophys. Res., 107, SSH 8-1
Basu, S., & Antia, H. M. 1995, MNRAS, 276, 1402
Bochsler, P. 2000, Rev. Geophys., 38, 247
Borrini, G., Gosling, J.T., Bame, S.J., & Feldman, W.C. 1983, Sol. Phys., 83, 367
Borrini, G., Gosling, J. T., Bame, S. J., Feldman, W. C., & Wilcox, J. M. 1981, J. Geophys. Res., 86, 4565
Bürgi, A. 1992, J. Geophys. Res., 97, 3137
Dusenbery, P. B., & Hollweg, J. V. 1981, J. Geophys. Res., 86, 153
Endev, E., Lie-Svendsen, Ø., Hansteen, V. H., & Leer, E. 2005, ApJ, 624, 402
Feldman, W. C., Asbridge, J. R., Bame, S. J., & Gosling, J. T. 1978, J. Geophys. Res., 83, 2177
Fisk, L. A. 2003, J. Geophys. Res., 108, SSH 7-1
Geiss, J. 1982, Space Sci. Rev., 33, 201
Geiss, J., Hirt, P., & Leutwyler, H. 1970, Sol. Phys., 12, 458
Guzik, J. A., & Cox., A. N. 1993, ApJ, 411, 394
Hansteen, H., Leer, E., & Holzer, T. E. 1994, ApJ, 428, 843
———. 1997, ApJ, 482, 498
Kasper, J. C., Lazarus, A. J., Steinberg, J. T., Ogilvie, K. W., & Szabo, A. 2006, J. Geophys. Res., 111, A03105
Laming, J. M. 2004, ApJ, 614, 1063
Levine, R. H., Altschuler, M. D., & Harvey, J. W. 1977, J. Geophys. Res., 82, 1061
Li, X., & Habbal, S. R. 2000, J. Geophys. Res., 105, 7583

Liewer, P. C., Neugebauer, M., & Zurbuchen, T. 2004, Sol. Phys., 223, 209
Marsch, E., Rosenbauer, H., Schwenn, R., Muehlhaeuser, K.-H., & Neubauer, F. M. 1982a, J. Geophys. Res., 87, 35
Marsch, E., Schwenn, R., Rosenbauer, H., Muehlhaeuser, K.-H., Pilipp, W., & Neubauer, F. M. 1982b, J. Geophys. Res., 87, 52
McComas, D. J., Elliott, H. A., Schwadron, N. A., Gosling, J. T., Skoug, R. M., & Goldstein, B. E. 2003, Geophys. Res. Lett., 30, 24
McKenzie, J. F., Ip, W.-H., & Axford, W. I. 1978, Nature, 274, 350
Neugebauer, M. 1976, J. Geophys. Res., 81, 78
———. 1981, Fundam. Cosm. Phys., 7, 131
Ogilvie, K. W., & Hirshberg, J. 1974, J. Geophys. Res., 79, 4595
Ogilvie, K. W., et al. 1995, Space Sci. Rev., 71, 55
Parker, E. N. 1958, ApJ, 128, 664
Press, W. H., Teukolsky, S. A., Vetterling, W. T., & Flannery, B. P. 2002, Numerical Recipes in C: The Art of Scientific Computing (2nd ed.; New York: Cambridge Univ. Press)
Schwadron, N. A., McComas, D. J., & DeForest, C. 2006, ApJ, 642, 1173
Steinberg, J. T., Lazarus, A. J., Ogilvie, K. W., Lepping, R., & Byrnes, J. 1996, Geophys. Res. Lett., 23, 1183
Tu, C.-Y., & Marsch, E. 2001, A&A, 368, 1071
Tu., C.-Y., Wang, L.-H., & Marsch, E. 2003, J. Geophys. Res., 108, SSH 9–1
von Steiger, R., Geiss, J., Gloeckler, G., & Galvin, A. B. 1995, Space Sci. Rev., 72, 71
Wang, Y.-M. 1994, ApJ, 437, L67
Wang, Y.-M., & Sheeley, N. R. 1990, ApJ, 355, 726
Woo, R., Habbal, S. H., & Feldman, U. 2004, ApJ, 612, 1171